

## Hadley Cell Dynamics in a Primitive Equation Model. Part II: Nonaxisymmetric Flow

HYUN-KYUNG KIM AND SUKYOUNG LEE

*Department of Meteorology, The Pennsylvania State University, University Park, Pennsylvania*

(Manuscript received 24 January 2000, in final form 8 February 2001)

### ABSTRACT

This paper investigates the effect of baroclinic eddies on the structure of the Hadley cell. Self-consistent calculations of both axisymmetric and nonaxisymmetric circulations allow an unambiguous estimate of baroclinic eddy effects on the structure of the Hadley cell. Furthermore, a diagnostic analysis allows us to partition the influence of baroclinic eddies into “direct” and “indirect” responses. The former refers to the meridional circulation attributable to the explicit eddy fluxes while the latter refers to the meridional circulation attributable to part of other processes, such as surface friction and diabatic heating changes, which are in fact induced by the baroclinic eddies. For a realistic parameter range, it is found that these indirect responses are comparable to the direct response.

While the direct response of the eddies is always found to be a strengthening of the Hadley cell, the indirect response can either strengthen or dampen the Hadley cell. When the thermal driving of the atmosphere is moderate, baroclinic eddies always amplify and broaden the Hadley cells. On the other hand, if the thermal driving over the Tropics and subtropics becomes sufficiently strong, the net effect of baroclinic eddies is to dampen (strengthen) the Hadley cell above (below) the height level of maximum diabatic heating. An explanation for this behavior is given in terms of competition between the Hadley cell driving by the eddy fluxes (both direct and indirect) and damping of the Hadley cell by potential temperature mixing.

### 1. Introduction

The relative role of extratropical eddy heat and momentum flux divergences in shaping the zonal mean meridional circulation (MMC) seems far from being clarified. Through the use of a linear diagnostic equation (e.g., Eliassen 1951; Kuo 1956; the MMC equation hereafter), there have been efforts to address this issue. In particular, Crawford and Sasamori (1981) and Pfeffer (1981) used the MMC equation to investigate the seasonal and annual mean MMC response to individual momentum and heat sources. Both studies suggest that the extratropical eddies play a minor role in maintaining the Hadley cell, as their calculations show that eddy fluxes drive only 20%–30% of the Hadley cell.

As stated by Chang (1996), and also in Part I of this study (Kim and Lee 2001, hereafter KL), the interpretation of the results of MMC equation diagnostics faces a potentially serious difficulty. This is because the premise of such a diagnostic analysis is that each momentum and heat source for the MMC is independent from each other. However, for a sufficiently long timescale, these source terms must influence one another (Chang 1996). For example, in this study, we will see that when the Hadley cells obtained from two model runs are compared, one run with eddies and the other without eddies,

it is found that 75% of the Hadley cell is ultimately driven by the eddy fluxes. That is, the ratio of the maximum meridional mass streamfunction obtained from the run without the eddies to that with the eddies is 0.25. Furthermore, the MMC diagnostics applied to these two model runs indicates that only 38% of the Hadley cell is directly attributable to the eddy fluxes, while the remaining 37% is attributable to other processes such as changes in diabatic heating and surface friction, which are in fact ultimately driven by the eddy fluxes. In other words, the heat and momentum sources of the MMC are not independent from each other; in this case, the eddy driven MMC alters the diabatic heating and surface friction sources in such a manner so as to drive an even stronger MMC.

Because of the ambiguity exemplified above, with the MMC equation diagnostics alone, it is difficult to estimate even the lowest order impact of the eddy fluxes on the Hadley cells in the atmosphere. It is this difficulty that motivated our study, and it is hoped that this study will help us to better understand the role played by the eddy fluxes for the Hadley circulation of the atmosphere. For this purpose, we adopt a strategy of combining the MMC equation diagnostics with primitive equation model calculations, both with and without baroclinic eddies. It should be noted that Becker et al. (1997) also compared the Hadley cells obtained from model simulations, with and without the baroclinic eddies. While such a comparison allows one to unambiguously determine the impact of eddy fluxes on the Hadley cell, it alone cannot

---

*Corresponding author address:* Dr. Sukyoung Lee, Dept. of Meteorology, The Pennsylvania State University, University Park, PA 16802.  
E-mail: sl@essc.psu.edu

be used to evaluate the processes through which the effect of the eddy fluxes manifest themselves. As we will show, by including MMC diagnostics, this study is able to further elucidate these physical processes.

The paper is organized as follows. Section 2 outlines the strategy of combining the numerical model experiments with the MMC equation diagnostics. Section 3 briefly describes the model and the analysis method. The main thrust of this paper is presented in section 4. The discussion and concluding remarks follow in section 5.

## 2. The strategy

We first integrate a primitive equation (PE) model forward in time, both with and without the baroclinic eddies. The former and latter solutions, respectively, are referred to as nonaxisymmetric and axisymmetric flows. We then perform the MMC diagnostics on the eddy-driven Hadley cell which can be readily obtained by subtracting the MMC in the axisymmetric flow from that in the nonaxisymmetric flow. This approach not only allows an unambiguous estimate of the effect of the eddy fluxes on the Hadley cell, but also partitions the eddy-driven Hadley cell into “direct” and “indirect” parts, providing further insight into the impact of the eddy fluxes.

In order to clarify the merit of this approach at the outset, it is useful to consider the diagnostic equation for the nonaxisymmetric flow written in symbolic form as

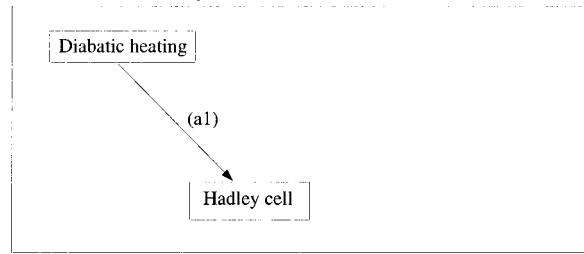
$$L\Psi^* = S, \quad (1)$$

where  $L$  and  $S$  represent the linear operator [(4) in KL] and the sum of the source terms [(6) in KL], respectively. The streamfunction response obtained from this diagnostic equation (i.e., the MMC equation) is denoted by  $\Psi^*$ , in distinction from the “true” streamfunction,  $\Psi$ , calculated by the PE model. We next write the linear operator, sources, and the streamfunction response into an axisymmetric part and a deviation, that is,  $L = L_a + L_e$ ,  $S = S_a + S_e$ , and  $\Psi^* = \Psi_a^* + \Psi_e^*$ , where the subscripts  $a$  and  $e$  denote the axisymmetric part of the flow and the corresponding deviation, respectively. It is crucial to note that the above partition between the axisymmetric and deviation from the axisymmetric part is not possible without *an explicit information of the axisymmetric, as well as the nonaxisymmetric circulation*. The linear operators  $L_a$  and  $L_e$  take the following forms:

$$L_a = \frac{R\Gamma_a}{a^2 p} \frac{\partial^2}{\partial \mu^2} + \frac{4\Omega^2 \mu^2}{(1 - \mu^2)} \frac{\partial^2}{\partial p^2}, \quad \text{and} \quad L_e = \frac{R\Gamma_e}{a^2 p} \frac{\partial^2}{\partial \mu^2},$$

where  $\Gamma_a = -\overline{T_a}(\partial \ln \overline{\Theta_a} / \partial p)$  is the static stability parameter and  $\overline{T_a}(p)$  and  $\overline{\Theta_a}(p)$  are the horizontally averaged temperature and potential temperature of the axisymmetric circulation, respectively. The  $\Gamma_e$  is obtained by subtracting  $\Gamma_a$  from  $\Gamma$ , where  $\Gamma$  takes the same form as  $\Gamma_a$  above, except that  $\overline{T_a}(p)$  and  $\overline{\Theta_a}(p)$  are replaced by the nonaxisymmetric counterparts. Thus, it is clear that

### Axisymmetric circulation



### Non-axisymmetric circulation

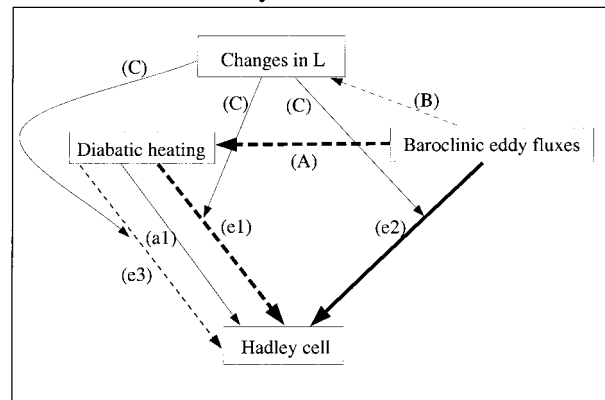


FIG. 1. Schematic representation of the MMC driving for (a) the axisymmetric and (b) the corresponding nonaxisymmetric flow.

$L_e$  is nonzero due to changes in static stability. Substituting these expressions into (1), and subtracting from (1) the equation for the axisymmetric flow, that is,

$$L_a \Psi_a^* = S_a, \quad (2)$$

one obtains an equation for an “eddy-driven” mass streamfunction:

$$\Psi_e^* = L^{-1}(S_e - L_e \Psi_a^*). \quad (3)$$

Furthermore, if we write the source term as  $S = F + SF + H$ , where the terms on the rhs correspond to eddy fluxes, surface friction, and diabatic heating, respectively, then we can write the eddy-driven source term  $S_e$  as  $F + SF_e + H_e$ , where  $SF_e$  and  $H_e$  are the eddy-driven sources of surface friction and diabatic heating. Thus,  $\Psi_e^*$  can be partitioned into *direct* (i.e.,  $L^{-1}F$ ) and *indirect* [i.e.,  $L^{-1}(SF_e + H_e - L_e \Psi_a^*)$ ] eddy responses. Note that by diagnosing the MMC of the nonaxisymmetric flow alone, the indirect response will be attributed to other physical processes, that is,  $SF$  and  $H$ , when in fact a substantial part of these processes are induced by the eddies. In addition, if  $\Psi_e^* \approx \Psi_e$ , and  $\Psi_a^* \approx \Psi_a$ , which we will find to be the case for most of our experiments, one can determine how much of the eddy-driven MMC,  $\Psi_e$ , obtained *unambiguously* from the PE model integrations, is attributable to each source

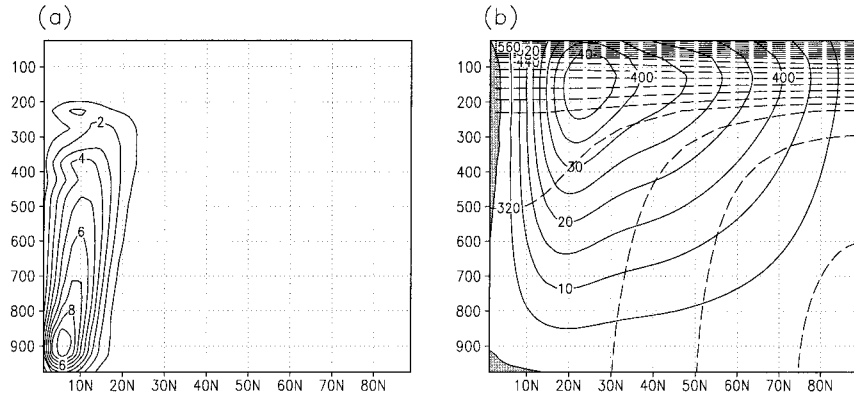


FIG. 2. Axisymmetric (a) mass streamfunction, (b) zonal wind (solid lines) and potential temperature (dashed lines) obtained by including the horizontal diffusion process for the control case. Contour interval in (a) is  $1 \times 10^9 \text{ kg s}^{-1}$  and in (b)  $5 \text{ m s}^{-1}$  and  $20 \text{ K}$ . Zero contours for (a) are omitted and the shaded area in (b) indicates the region of easterlies.

term within  $S_e$  and to changes in the static stability ( $L_e \Psi_a^*$ ).

It should be noted that the diagnosed *direct* eddy response,  $L^{-1}F$ , also includes an *indirect* contribution as well. For example, surface friction is able to alter the eddy fluxes,  $F$ , both by changing the eddy structure itself and by changing the zonal mean flow, which in turn influences the eddy fluxes. As in KL, because the results shown in this study imply that there is no cancellation between the *hidden*<sup>1</sup> indirect response within  $L^{-1}F$  and the *diagnosed* indirect response,  $L^{-1}(SF_e + H_e - L_e \Psi_a^*)$ , the latter can be viewed as a conservative estimate of the indirect response.

The essence of the above idea may be summarized by the schematic diagram shown in Fig. 1. In this figure, the boxes identify processes or phenomena, and the arrows denotes the direction of the influence between these processes/phenomena. In order to keep the argument as simple as possible, suppose that there are only two sources for the Hadley cell: diabatic heating and baroclinic eddy (heat and momentum) fluxes. In this hypothetical case, for an axisymmetric flow (Fig. 1a), the diabatic heating is the only driving mechanism for the Hadley cell:

$$L_a \Psi_a^* = S_1, \tag{4}$$

where  $S_1$  represents diabatic heating  $[(\Theta_E - \Theta)/\tau]$ . The arrow denoted by a1 indicates this process. Now suppose that the same axisymmetric circulation is perturbed by baroclinic eddies, while holding the external diabatic heating parameters ( $\Theta_E$  and  $\tau$ ) fixed. The resulting sta-

<sup>1</sup> In analogy to KL, we consider calculating a steady state solution for nonaxisymmetric flow, while artificially ensuring that all other *source* terms remain fixed at their unperturbed values in the initial axisymmetric flow. The difference between  $\Psi$  in this state and that in the unperturbed, axisymmetric run may be regarded as the *true* direct response to the eddies. The *hidden* indirect response can then be obtained by subtracting this *true* direct response from the “direct” response.

tistical steady state, nonaxisymmetric circulation is illustrated schematically in Fig. 1b. Now consider the MMC diagnostic equation,

$$L\Psi^* = S_1 + S_{1e} + F, \tag{5}$$

where  $F$  represents the eddy fluxes, and  $S_{1e}$  the changes in the diabatic heating (i.e.,  $-\delta\Theta/\tau$ ) that resulted from including the eddy fluxes. The arrow A represents the process that generates the  $S_{1e}$  term. For a sufficiently short timescale, the process A must be negligible. However, for a long timescale, the process A may not be ignored, and in fact can be substantial. Thus, if one is given a nonaxisymmetric circulation with *no* information about its axisymmetric counterpart (Fig. 1a), and uses the MMC equation diagnostic equation (5), then one would end up attributing the MMC response to  $S_1 + S_{1e}$  as being due to diabatic heating, when in fact the portion represented by  $S_{1e}$  is induced by the eddy fluxes.

In order to help grasp a more complete picture of the various nonlinear interactions, we first note that changes in  $\Theta$  made by the eddy fluxes must also change the linear operator,  $L$  (see arrow B in the Fig. 1b). A derivation, analogous to that that led to (3), gives

$$(L_a + L_e)\Psi_e^* = S_{1e} + F - L_e \Psi_a^*. \tag{6}$$

We are now able to make a one-to-one correspondence between the individual responses in (6) and the processes denoted by arrows e1, e2, and e3:

- e1 is a solution to  $(L_a + L_e)\Psi_e^* = S_{1e}$ ;
- e2 is a solution to  $(L_a + L_e)\Psi_e^* = F$ ;
- e3 is a solution to  $(L_a + L_e)\Psi_e^* = -L_e \Psi_a^*$ ; and
- a1 is still the solution to  $L_a \Psi_a^* = S_1$ .

The process e3 represents the change in the MMC response attributable to the change in  $L$  (via process C) in response to the original diabatic heating,  $S_1$ , that is, the solution to  $L_a \Psi^* = S_1$ . Comparing Figs. 1a and 1b, it is clear that the processes denoted by arrows e1, e2, and e3 are ultimately driven by the eddy fluxes. In

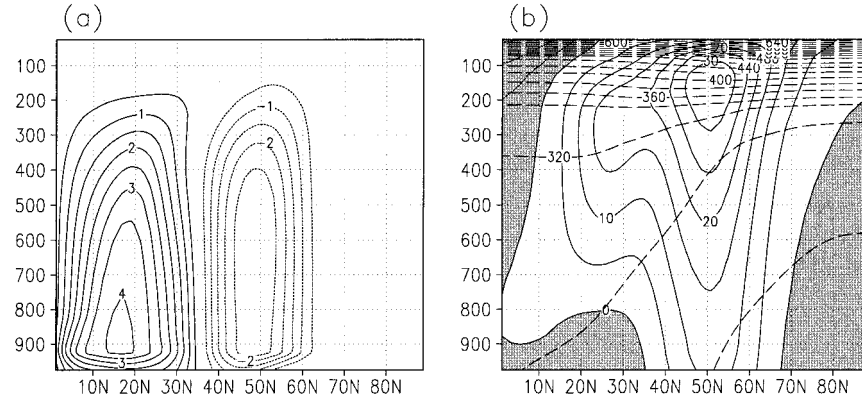


FIG. 3. Nonaxisymmetric (a) mass streamfunction, (b) zonal wind (solid lines) and potential temperature (dashed lines) in the control case. Contour interval in (a) is  $5 \times 10^9 \text{ kg s}^{-1}$  and in (b) is  $5 \text{ m s}^{-1}$  and  $20 \text{ K}$ . In (a), dotted lines indicate negative values and zero contours are omitted. The shaded area in (b) indicates the region of easterlies.

particular, we emphasize that for the nonaxisymmetric circulation (Fig. 1b), the response to the diabatic heating includes three different components:  $a1$ ,  $e1$ , and  $e3$ . As stated above, if one is to diagnose just the nonaxisymmetric circulation with *no knowledge of the axisymmetric counterpart*, then one would erroneously interpret  $a1 + e1 + e3$  as the response to the diabatic heating when in fact  $e1 + e3$  are ultimately driven by the eddies; only  $e2$  would be attributed to the eddy fluxes. As shown above, by comparing the *two* steady states with the MMC diagnostics, we are not only able to discern how much of the MMC is ultimately driven by the eddy fluxes, but are also able to quantify through what processes the eddy fluxes manifest itself (e.g.,  $e1$  and  $e3$ ).

As stated in the introduction, in one of our experiments, only 38% of the Hadley cell strength is explicitly attributed to the eddy fluxes; that is, the maximum value of  $L^{-1}F$  is 38% that of  $\Psi^*$ . However, the diagnosis outlined above indicates that the eddy-driven diabatic heating,  $H_e$ , and the surface friction,  $SF_e$ , account for nearly 37% of the total Hadley cell strength. Clearly, either  $\Psi_e$  (e.g., Becker et al. 1997) or the response to  $F$  (Crawford and Sasamori 1981; Pfeffer 1981), alone, is unable to yield such information. Because  $\Psi_a$  is never realized in the atmosphere, we believe that the above analysis will be proven to be fruitful for gaining insight into the role of eddies for driving the Hadley cells in the atmosphere.

### 3. Model and the diagnostic equation

Because the model and MMC equation to be used in this paper are described in detail in KL, a brief description of their properties is summarized here.

In the PE model of this study, there are 20 equally spaced sigma levels and the horizontal scale is truncated at rhomboidal 30. The model is forced by relaxing toward a radiative convective equilibrium potential temperature profile,  $\Theta_E$ :

$$\frac{d\Theta}{dt} \propto -\frac{1}{\tau}(\Theta - \Theta_E),$$

where  $\tau$  is the radiative relaxation timescale. In this study, three different values of  $\tau$  are used: 4, 20, and 40 days. The  $\Theta_E$  takes the form of

$$\frac{\Theta_E(\theta, \sigma)}{\Theta_0} = 1 - \frac{1}{3}\Delta_h(3 \sin^2\theta - 1) - \Delta_v\left(\frac{h}{H_s} \ln\sigma + \frac{1}{2}\right),$$

where  $\theta$  is latitude;  $\Theta_0$  the global mean value of  $\Theta_E$ ; and  $\Delta_h$  and  $\Delta_v$  the fractional change in  $\Theta_E$  from equator to Pole, and from the tropopause to surface, respectively. However, for one particular run, the model is also forced by an additional constant heating,  $Q_c$ , which is used to crudely represent convection in the Tropics. Following Becker et al. (1997),  $Q_c$  is defined as

$$\frac{Q_c}{Q_{\max}} = \begin{cases} \exp\left[-\frac{(p - p_0)^2}{2\sigma_p^2}\right] \times \cos^2\left[\frac{\pi(\theta - \theta_0)}{\sigma_\theta}\right] & \text{for } |\theta - \theta_0| < \sigma_\theta \\ 0 & \text{otherwise,} \end{cases}$$

where  $Q_{\max} = 2 \text{ K day}^{-1}$ ,  $p_0 = 525 \text{ mb}$ ,  $\sigma_p = 200 \text{ mb}$ ,  $\theta_0 = 0^\circ$ , and  $\sigma_\theta = 20^\circ$ . As stated by Becker et al. (1997),

an addition of  $Q_c$  to the expression for the relaxation toward  $\Theta_E$  is equivalent to relaxation toward  $\Theta_E + \tau Q_c$ ,

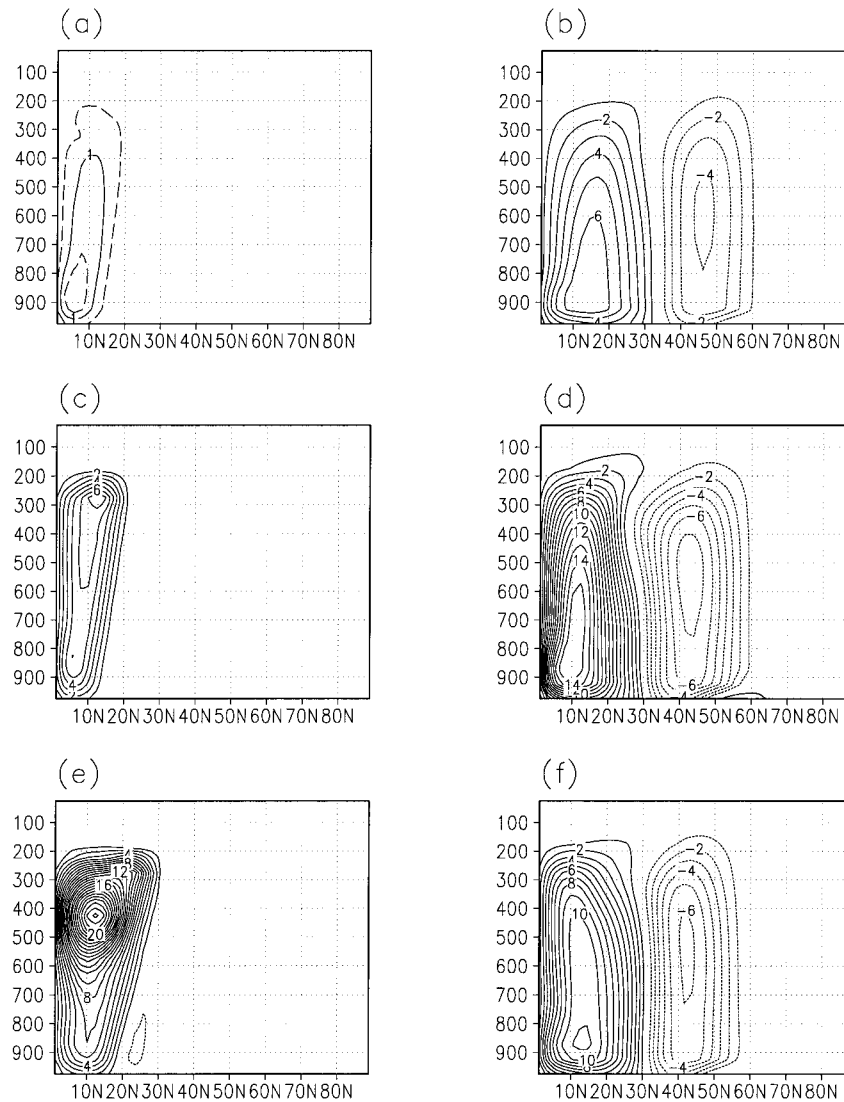


FIG. 4. Mass streamfunctions of the case with  $\tau = 20$  days for (a) axisymmetric and (b) nonaxisymmetric flows, with  $\tau = 4$  days for (c) axisymmetric and (d) nonaxisymmetric flows, and with additional tropical heating,  $Q_e$ , for (e) axisymmetric and (f) nonaxisymmetric flows. Contour interval is  $1 \times 10^{10} \text{ kg s}^{-1}$ . Additional contours ( $5 \times 10^9 \text{ kg s}^{-1}$ ) are used for (a) (dashed lines). Dotted lines indicate negative values and zero contours are omitted.

where  $\tau$  denotes the relaxation timescale. Because the diabatic heating field is symmetric across the equator, without sampling error, one expects cross equatorial symmetry. Therefore, we only display the results for one hemisphere.

The model is subjected to viscosity and conductivity, represented by vertical diffusion of momentum and potential temperature, respectively. Additional damping includes surface friction and scale-selective horizontal diffusion. We find that an eighth-order horizontal diffusion formulation serves this purpose well, as it has a negligible effect on the axisymmetric circulation. The value of the horizontal diffusion coefficient is set to  $8$

$\times 10^{37} \text{ m}^8 \text{ s}^{-1}$ . The precise form of other model parameters, as well as their values, are provided by KL.

The MMC equation (1) is obtained under the assumption of zonal symmetry and quasigeostrophy. Again, a full description of this equation can be found in KL, Haynes and Shepherd (1989), and Plumb (1982).

#### 4. Nonaxisymmetric circulation

##### a. Do eddy fluxes drive or dampen the Hadley cell?

In order to attribute circulation differences between the axisymmetric and nonaxisymmetric flows to the eddy fluxes, it is necessary to ensure that the horizontal

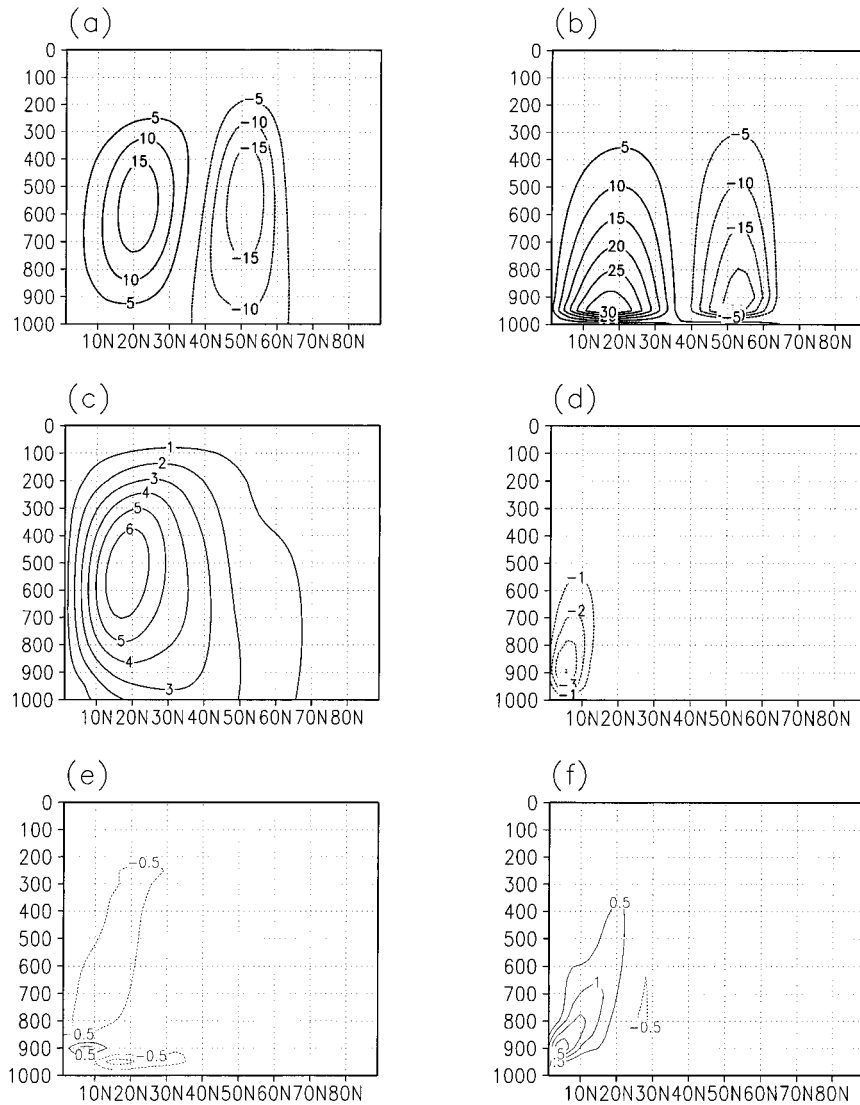


FIG. 5. For a control nonaxisymmetric flow, the QG diagnostic mass streamfunction responses to (a) eddy fluxes ( $F^M + F^H$ ), (b) eddy surface friction ( $SF_e$ ), (c) eddy diabatic heating ( $H_e$ ), (d) eddy-induced static stability change on the axisymmetric circulation ( $L_e \Psi_a$ ), (e) eddy part of vertical mixing of zonal momentum ( $D_e^U$ ), (f) eddy part of vertical mixing of enthalpy ( $D_e^E$ ), and (g) total eddy forcings. (h) The total eddy-driven mass streamfunction from the PE model. Contour interval is  $5 \times 10^9 \text{ kg s}^{-1}$  for (a), (b), (g), and (h);  $1 \times 10^9 \text{ kg s}^{-1}$  for (c) and (d); and  $5 \times 10^8 \text{ kg s}^{-1}$  for (e) and (f). Dotted lines indicate negative values and zero contours are omitted.

diffusion does not appreciably change the essential features of the axisymmetric circulation. Figures 2a and 2b show the mass streamfunction,  $\Psi$ , and the corresponding zonal wind and potential temperature fields of the axisymmetric circulation with the horizontal diffusion included. Compared with Figs. 2a and 2b in KL where horizontal diffusion is absent, the maximum velocity of the subtropical jet is reduced by 10% and there is a hint of a small-scale meridional cell developing in the equatorial upper troposphere. However, overall, this highly scale-selective diffusion does not seem to alter the axisymmetric flow in any appreciable manner.

Figure 3 shows the statistically steady state for the nonaxisymmetric flow with the control parameters [see section 4b(1)]. Considering the simple parameterization for diabatic heating and mechanical damping, the structure of the zonal mean zonal wind (Fig. 3b) seems reasonable, in particular when compared with equinoctial conditions in the Southern Hemisphere (SH); both the subtropical and eddy-driven (i.e., polar front) jets can be seen at  $30^\circ$  and  $50^\circ$  latitude, respectively, and as expected, the former jet is much weaker than its counterpart in the axisymmetric flow (cf. Figs. 2b and 3b). However, it is important to remind the reader that our

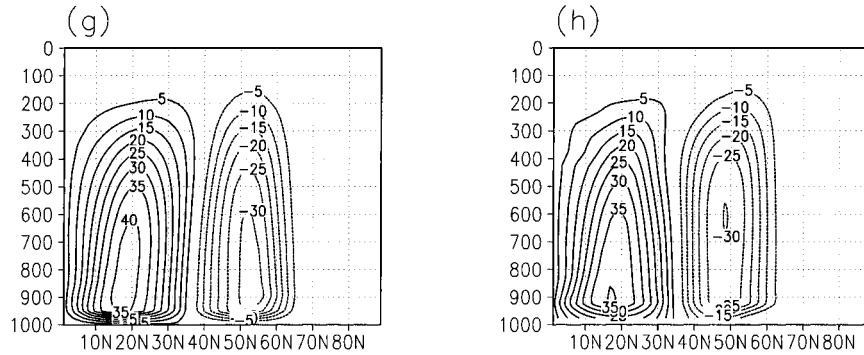


FIG. 5. (Continued)

goal is to gain insight into the driving mechanisms of the Hadley cell, rather than simply simulating the observed Hadley cell as well as one could. Therefore, we regard our circulation reasonable as long as the value of the maximum  $\Psi$  is within the range of observed values (e.g., see Peixoto and Oort 1992; Oort and Rasmusen 1970).

In the control case, in addition to driving the Ferrel cell, the presence of baroclinic eddies dramatically increases both the width and the strength of the Hadley cell (cf. Figs. 2a and 3a, and note the contour interval difference). Although not shown, we calculated both the annual mean and monthly mean MMCs using the National Centers for Environmental Prediction–National Center for Atmospheric Research (NCEP–NCAR) reanalysis dataset, which covers the years from 1958 to 1997. It is found that the maximum value of the mass streamfunction for the annual mean is  $8 \sim 9 \times 10^{10} \text{ kg s}^{-1}$ , while that during the month of April, which is close to equinox conditions, is  $9 \sim 10 \times 10^{10} \text{ kg s}^{-1}$ . The difference between the annual mean and the April mean values is much smaller than that shown by an earlier analysis (Oort and Rasmusen 1970; also see Fig. 1 of Lindzen and Hou 1988) where the data was relatively limited both in quantity and quality. The maximum value of the mass streamfunction in the nonaxisymmetric control run is  $4 \times 10^{10} \text{ kg s}^{-1}$ , a factor of 2.5 smaller than the NCEP–NCAR reanalysis April mean value. This discrepancy is primarily due to the use of a rather large value of  $\tau$ , 40 days. Decreasing the value of  $\tau$  to 20 days, we obtain the MMC whose strength is more in line with the observations (see Fig. 4b). Defining an amplification factor as the ratio of the maximum value of  $\Psi$  in the nonaxisymmetric circulation to that in the corresponding axisymmetric circulation, the amplification factor for the  $\tau = 20$  day case is 4 (cf. Figs. 4a and 4b). Although this value is lower than 5, obtained for the control case, it clearly demonstrates that the net effect of eddy fluxes is to significantly increase the strength of the Hadley cell. When the value of  $\tau$  is decreased to 4 days, the amplification factor is 3 (cf. Figs. 4c and 4d). Because computational stability requires a very short time step for even lower values of

$\tau$ , no additional experiments were performed. However, this set of experiments indicates that, to the extent that diabatic heating can be represented with relaxation toward “radiative–convective” equilibrium, over a wide range of values for  $\tau$ , the net effect of the eddy fluxes is to substantially strengthen the Hadley cell.

In contrast, when a sufficiently strong, constant heating,  $Q_c$  (see section 2), is added to the diabatic heating, the net effect of the eddy fluxes is to damp the Hadley cell above the level of the maximum  $Q_c$ , and strengthen the Hadley cell below the level of the maximum  $Q_c$  (cf. Figs. 4e and 4f and also see Fig. 9b). This result is consistent with the finding of Becker et al. (1997), and indicates that the eddy fluxes can either drive or damp the Hadley cell, depending on the form of the diabatic heating. Recalling that the addition of  $Q_c$  is equivalent to replacing  $\Theta_E$  with  $\Theta_E + \tau Q_c$ , because  $Q_c$  is concentrated in the vicinity of the equator, the addition of  $Q_c$  amounts to increasing the meridional gradient of the equilibrium potential temperature in the Tropics and subtropics.

## b. Direct versus indirect eddy driving of MMC

### 1) CONTROL CASE

The parametric values for the control case are identical to those given by KL. Specifically, the equilibrium potential temperature difference between the equator and Pole,  $\Theta_0 \Delta_n$ , and that between the tropopause and the surface,  $\Theta_0 \Delta_s$ , are 60 and 12.5 K respectively, and radiative relaxation timescale,  $\tau$ , is 40 days. As stated earlier, this value is somewhat long; however, as we will show below, essentially the same conclusions can be drawn for  $\tau = 20$  days, indicating that the main results of this paper are rather insensitive to the value of  $\tau$ .

Although nearly 75% of the total Hadley cell is unambiguously driven by the eddy fluxes (compare Figs. 2a and 3a), the direct response to the eddy momentum and heat fluxes explains only  $\sim 35\%$  of the “eddy-driven” Hadley cell (compare Figs. 5a and 5g). The latter value compares reasonably well with the observations (e.g., Pfeffer 1981). Note that the total  $\Psi_c^*$  (Fig. 5g), that is, the

solution to (3) with all source terms included, closely resembles  $\Psi_e$  (Fig. 5h), which is obtained by subtracting the mass streamfunction of the axisymmetric run from that of the nonaxisymmetric run, allowing us to proceed with the analysis outlined in section 2. In the annual mean, the maximum value of the mass streamfunction associated with the Hadley cell is  $\sim 6 \times 10^{10} \text{ kg s}^{-1}$  (Fig. 7.19 of Peixoto and Oort 1992), while the eddy fluxes account for  $\sim 2 \times 10^{10} \text{ kg s}^{-1}$  (Fig. 6 of Pfeffer 1981), about 33% of the total which is similar value to that obtained in our model runs. Thus, to the extent that the above PE model captures the essential dynamics in the atmosphere, it is tempting to conclude that 75%, rather than 35%, of the Hadley cell strength in the atmosphere is, in fact, driven by the midlatitude eddy fluxes. However, as stated earlier, if the atmospheric tropical diabatic heating is better represented by the addition of a sufficiently strong, constant heating, that is,  $Q_c$ , we must conclude that above the level of the maximum heating the net effect of the eddy fluxes is to dampen the Hadley cell. This point will be revisited in section 4b(3). We now try to interpret the indirect effects of the eddies, for example, the MMC response to the surface friction (Fig. 5b) and diabatic heating changes (Figs. 5c and 5d) using the following stepwise argument.

We interpret the structure of the MMC response to the eddy-induced surface friction,  $SF_e$ , by first assuming that the zonal momentum equation at the surface is represented by a balance between surface friction and the Coriolis torque, and noting that the eddy fluxes must directly induce surface westerlies in midlatitudes and surface easterlies in the Tropics and subtropics. Therefore, the role of surface friction must be to increase (decrease) the vertical shear in the midlatitudes (Tropics and subtropics), inducing an additional indirect (direct) circulation (see Fig. 5b). Although there is no equivalent analysis for the observations that one can compare with, the magnitude of the friction-driven MMC seems surprisingly large. If one is only to diagnose the nonaxisymmetric flow MMC, there is no way to separate  $SF_e$  from  $SF_a$ , and thus the impact of  $SF_e$  will be unknown. Because  $SF_e$  is induced by the eddies, the resulting MMC should be interpreted as an indirect response to the eddy fluxes. Using the Ferrel cell as an example, Chang (1996) demonstrates this very point. In contrast to surface friction, we find that the effect of both the viscosity (Fig. 5e) and thermal conductivity (Fig. 5f) on the eddy-driven Hadley cell to be minimal.

Perhaps more subtle, potentially important indirect effects of the eddy fluxes are represented by  $H_e$  and  $L_e\Psi_a$  [see (3)]. As will be elaborated below, the former represents eddy-induced diabatic heating (Fig. 5c), while the latter represents the effect of eddy-induced static stability changes from the axisymmetric circulation (Fig. 5d). Given that the response to the baroclinic eddy fluxes is a thermally direct cell in the Tropics and subtropics (see Fig. 5a), there must be eddy-induced diabatic heating in the deep Tropics, which further strengthens the Hadley cell. On the other hand, the eddy

fluxes tend to increase the static stability, which then weakens the Hadley cell (see Fig. 5d). Because the direct cell attributable to  $H_e$  is much stronger than the indirect cell attributable to  $L_e\Psi_a$ , the net effect of these two processes is to intensify the Hadley cell.

## 2) CASES WITH SHORTER RADIATIVE RELAXATION TIMESCALES

The analysis of the control case shows that the indirect eddy response is greater than the direct eddy response. One important factor behind this behavior is that the damping of the Hadley cell due to the eddy-induced static stability change,  $L_e\Psi_a$ , is overwhelmed by the strengthening of the Hadley cell by the eddy-induced diabatic heating,  $H_e$ . Because these processes are driven by the eddy fluxes, whose action on the general circulation is nontrivial to predict, it is not immediately obvious whether the same picture will hold for a more strongly forced atmosphere.

Although there are some differences, it turns out that essentially the same conclusion can be drawn for cases with stronger radiative forcing, that is, those for  $\tau = 20$  and 4 days. For example, the ratio of  $\Psi_{\max}$  for  $L_e\Psi_a$  to that for  $H_e$  is close to  $-0.5$  for all three cases (cf. Figs. 5c and 5d; Figs. 6c and 6d; Figs. 7c and 7d), where  $\Psi_{\max}$  denotes the maximum value of  $\Psi$ . The ratio of  $\Psi_{\max}$  for  $H_e$  to that for the eddy fluxes,  $F^M + F^H$ , is 0.4, 0.45, and 0.6 for the control,  $\tau = 20$  day, and  $\tau = 4$  day cases, respectively (cf. Figs. 5c and 5a; Figs. 6c and 6a; Figs. 7c and 7a), a rather moderate increase.

The contribution of the eddy-driven surface friction to the Hadley cell also shows insensitivity to the value of  $\tau$ . As can be inferred from Figs. 5b, 6b, and 7b, for all three cases, the ratio of  $\Psi_{\max}$  for  $SF_e$  to that for  $F^M + F^H$  is about 2. For these analyses, we continue to assume that  $\Psi_e^* \approx \Psi_e$ , and this is indeed the case (cf. Figs. 6e and 6f for  $\tau = 20$  day, and Figs. 7e and 7f for  $\tau = 4$  day runs).

## 3) EFFECT OF THE "CONVECTIVE HEATING," $Q_c$

As can be inferred from the discussion in section 4a and the results from the above section, the additional convective heating,  $Q_c$ , must alter the above picture that the effect of  $H_e$  dominates that of  $L_e\Psi_a$ . Before discussing the nonaxisymmetric model results with nonzero  $Q_c$ , we first examine the influence of nonzero  $Q_c$  on the axisymmetric solution. It is found for the axisymmetric model with nonzero  $Q_c$  that the Hadley cell is much stronger than that observed (Fig. 4e). For such a strong meridional circulation, it is expected that the quasigeostrophic (QG) approximation is seriously violated. Not surprisingly,  $\Psi_a^*$  is no longer a good approximation of  $\Psi_a$ , as the former is much weaker than the latter, in particular in the upper troposphere.

For this axisymmetric flow, we offer an explanation for the above discrepancy between the diagnosed and

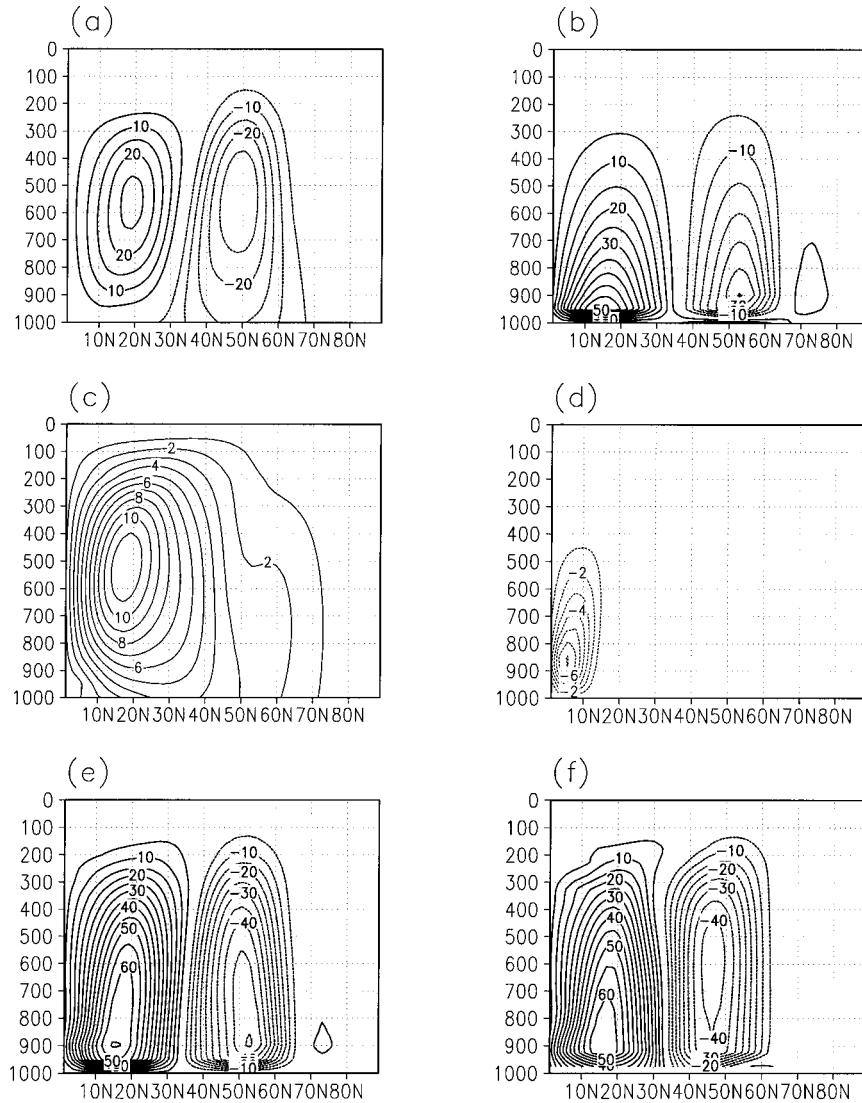


FIG. 6. For the case with  $\tau = 20$  days, the QG diagnostic mass streamfunction responses to (a) eddy fluxes, (b) eddy surface friction, (c) eddy diabatic heating, (d) eddy-induced static stability change on the axisymmetric circulation, and (e) total eddy forcings. (f) The total eddy-driven mass streamfunction from the PE model. Contour interval is  $5 \times 10^9 \text{ kg s}^{-1}$  for (a), (b), (e), and (f) and  $1 \times 10^9 \text{ kg s}^{-1}$  for (c) and (d). Dotted lines indicate negative values and zero contours are omitted.

the PE model's Hadley cell by considering the QG approximation, together with an examination of the Hadley cell structure (see Fig. 4e). The QG approximation for the thermodynamic energy equation amounts to neglecting meridional advection of  $\bar{\Theta}$  by the zonal mean meridional wind,  $\bar{v}(\partial\bar{\Theta}/\partial y)$ , where the overbar denotes a zonal mean. As can be seen in Fig. 4e, because the Hadley cell tilts poleward with height in the upper troposphere, given that  $\partial\bar{\Theta}/\partial z > 0$  and  $\partial\bar{\Theta}/\partial y < 0$ , one expects  $\bar{v}(\partial\bar{\Theta}/\partial y)$  to be of opposite sign to that of  $\bar{w}(\partial\bar{\Theta}/\partial z)$ . In other words, there must be partial cancellation between these two terms. Therefore, if the meridional advection term is ignored, a weaker vertical

wind speed will suffice to balance the diabatic heating. Thus, we infer that the larger amplitude of the meridional temperature gradient in the Tropics, which results from the addition of  $Q_c$ , will lead to a feeble QG-diagnosed Hadley cell, and this is indeed the case (not shown). In fact, Fig. 8a shows that in the axisymmetric flow, the vertically integrated  $\bar{\Theta}$  exhibits a strong (compared to the nonaxisymmetric case) meridional temperature gradient in the subtropics. For reference, the vertically integrated  $\bar{\Theta}_E$  is also displayed in the same figure. Note that because of the nonzero  $Q_c$  in the Tropics, the vertically integrated potential temperature for both the axisymmetric and nonaxisymmetric flows are much

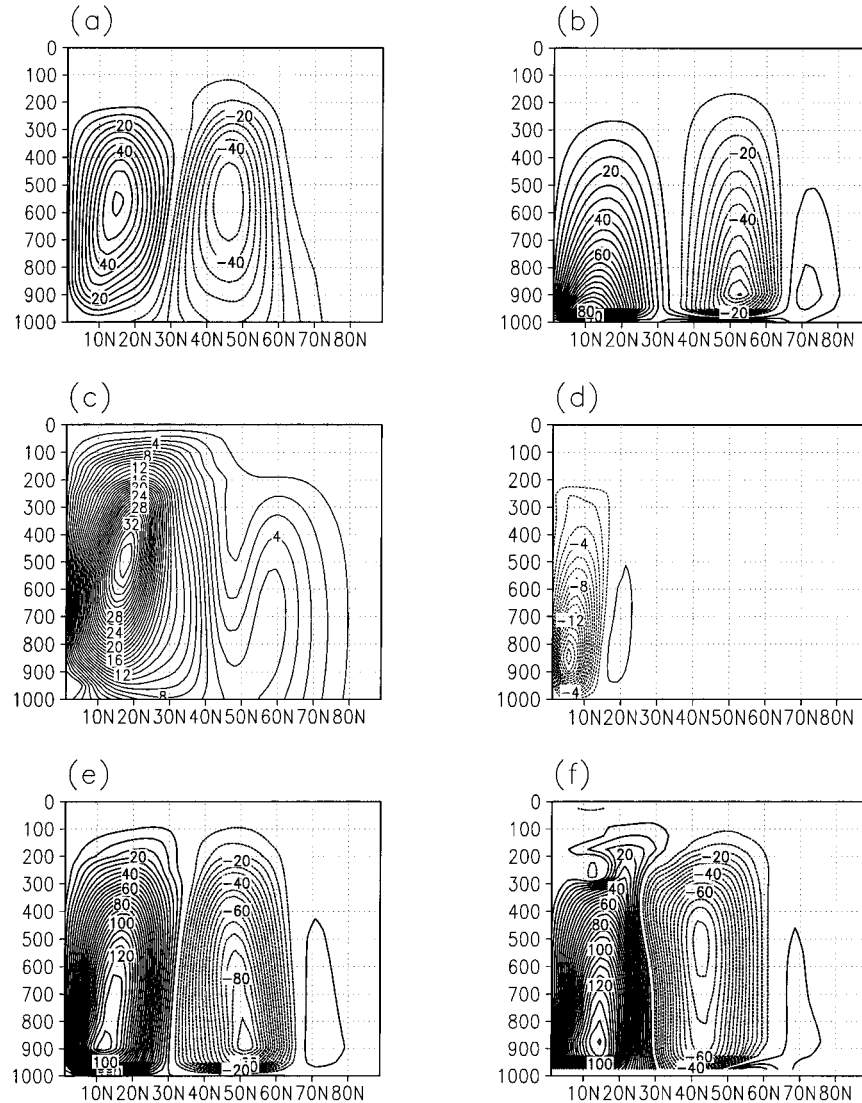


FIG. 7. As in Fig. 6 except for the case with  $\tau = 4$  days.

greater<sup>2</sup> than that of the control case. Figure 8a also shows that a substantial portion of this temperature gradient is removed in the nonaxisymmetric flow, presumably through mixing by the eddy fluxes. Consistent with this much weakened meridional temperature gradient,

<sup>2</sup> By the thermal wind relation, in the Tropics,  $\partial\bar{u}/\partial z$  must be greater for the nonzero  $Q_c$  case. Assuming that the surface zonal wind remains small, this indicates that in the tropical and subtropical upper troposphere,  $\partial\bar{u}/\partial y$  must also be greater for the nonzero  $Q_c$  case, which was indeed found to be the case (not shown). In fact, in the inviscid limit,  $\partial\bar{u}/\partial y = f$ , as angular momentum is conserved along the upper branch of the Hadley cell. Because  $\partial\bar{u}/\partial y$  is ignored in QG diagnostics, this may also explain the discrepancy between  $\Psi_a$  and  $\Psi_a^*$ . However, noting that the neglect of  $\partial\bar{u}/\partial y$  is dynamically consistent with the neglect of  $\partial\bar{\theta}/\partial y$ , we prefer to think of the discrepancy in terms of the latter. This is because while it is straightforward to interpret the mixing of  $\bar{\theta}$  by eddy heat fluxes, a similar interpretation cannot be applied to  $\bar{u}$  and the eddy momentum flux.

for the nonaxisymmetric flow, the diagnosed Hadley cell,  $\Psi^*$ , agrees very well with the PE model's Hadley cell (compare Figs. 4f and 9a).

Keeping the above scaling arguments in mind, we attempt to offer an explanation for the effect of the eddies on the Hadley cell in the presence of nonzero  $Q_c$ . Because the diagnosed MMC is able to capture the nonaxisymmetric PE model's MMC (compare Figs. 4f and 9a) reasonably well, that is,  $\Psi \approx \Psi^*$ , it follows that  $\Psi_a + \Psi_e \approx \Psi_a^* + \Psi_e^*$ . Rearranging these terms yields the relationship

$$\Psi_e - \Psi_e^* \approx \Psi_a^* - \Psi_a, \quad (7)$$

indicating that  $\Psi_e^*$  must be a poor representation of  $\Psi_e$  since there is a large discrepancy between  $\Psi_a^*$  and  $\Psi_a$ . Therefore (3), by itself, is no longer useful for diagnosing  $\Psi_e$ . Instead, by substituting (3) into (7), we obtain

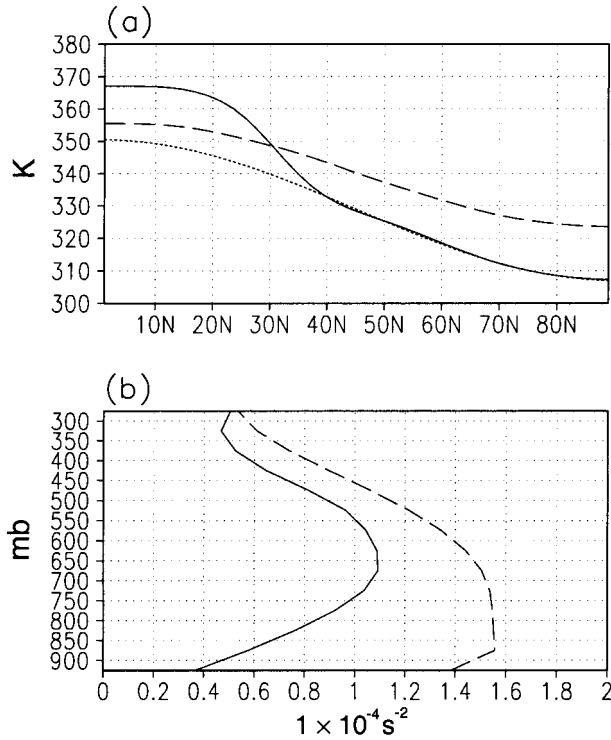


FIG. 8. (a) Vertically averaged radiative-convective equilibrium potential temperature (dotted line) and vertically averaged potential temperature for axisymmetric flow (solid line) and nonaxisymmetric flow (dashed line) for the case with nonzero  $Q_c$ . (b) Vertical profile of static stability averaged between  $0^\circ$  and  $30^\circ\text{N}$  for axisymmetric flow (solid line) and nonaxisymmetric flow (dashed line).

$$\Psi_e \approx L^{-1}(S_e - L_e\Psi_a) + (\Psi_a^* - \Psi_a). \quad (8)$$

Recalling the argument given above that the discrepancy between the diagnosed and actual MMC,  $\Psi_a^* - \Psi_a$ , stems from the large value of  $\partial\bar{\Theta}/\partial y$ , we interpret  $\Psi_a^* - \Psi_a$  as representing the effect of meridional mixing of  $\bar{\Theta}$  by the eddy fluxes. In other words,  $\Psi_a^* - \Psi_a$  is proportional to the difference in  $\partial\bar{\Theta}/\partial y$  between the axisymmetric and nonaxisymmetric flows, which results from the eddy mixing in the latter flow. A strong meridional mixing of  $\bar{\Theta}$  will also increase the static stability in the Tropics. Indeed, Fig. 8b shows that the eddy fluxes increase the static stability by as large as a factor of 3. Consistent with such a large change in static stability,  $L_e\Psi_a$  (Fig. 9e) plays a more important role than does  $H_e$  (Fig. 9d). This is in contrast to the cases with  $Q_c = 0$ , as described earlier. However, the greater contributor to the Hadley cell damping above the level of maximum heating is the process represented by the last two terms in (8) (see Fig. 9f).

Thus, although the direct response to the eddy fluxes,  $F^M + F^H$ , is to strengthen the Hadley cell (Fig. 9c), through the meridional mixing of  $\bar{\Theta}$ , the net effect of the eddy fluxes is to dampen the Hadley cell in the upper troposphere. Again, diagnostic analysis of the nonaxisymmetric circulation alone would lead to a misleading

conclusion that the eddy fluxes strengthen the Hadley cell, rather than dampen it.

## 5. Discussion and concluding remarks

From a direct comparison between the Hadley cells in both axisymmetric and nonaxisymmetric PE model calculations, and from a set of diagnostic analyses of the MMC, this study provides insight into the dynamical and thermodynamical processes of the Hadley cell.

When diabatic heating in the model is represented solely by a relaxation toward radiative-convective equilibrium, the net effect of the eddy fluxes is found to be a strengthening the Hadley cell. The fractional increase in the Hadley cell strength by the eddies depends on the radiative relaxation timescale,  $\tau$ , however, its sensitivity to  $\tau$  is rather modest. For the case of  $\tau = 20$  days, which shares many similarities with the atmosphere, the nonaxisymmetric Hadley cell is four times stronger than the axisymmetric Hadley cell, implying that  $\approx 75\%$  of the nonaxisymmetric flow's Hadley cell is ultimately driven by the eddies. However, the MMC diagnostics show that the direct response to the eddy fluxes account for only 38% of the nonaxisymmetric Hadley cell's strength, and the remaining 37% is attributable to other processes such as changes in diabatic heating and surface friction when in fact they are ultimately driven by eddy fluxes. As stated in the introduction, the diagnosis by Pfeffer (1981) (see Fig. 6 in that paper), along with the statistics of Peixoto and Oort (1992), suggest that for the annual mean, consistent with the case we just described, the eddy fluxes directly explain about 30% of the strength of the observed Hadley cell. Thus, it is tempting to conclude that in the atmosphere a much bigger portion of the Hadley cell is driven by the eddies than what was indicated by the analysis of Pfeffer (1981).

However, when a sufficiently strong, constant, diabatic heating is added in the tropics (note again that this is equivalent to increasing the meridional gradient of the equilibrium potential temperature in the Tropics and subtropics), the net effect of the eddy fluxes is to dampen the Hadley cell in the upper troposphere, above the level of maximum heating. This is because the changes in the  $\bar{\Theta}(y, \sigma)$  field by the eddy fluxes, which increase the static stability and decrease the meridional temperature gradient, significantly weaken the MMC response. This damping effect (see arrow e3 in Fig. 1b) dominates the increased eddy fluxes and the eddy-induced diabatic heating (see arrows e2 and e1 in Fig. 1b) and surface friction changes that amplify the Hadley cell. Again, a diagnostic analysis on the nonaxisymmetric flow alone cannot identify these complex, indirect actions of the eddies. In fact, such an analysis would tell us that the eddy fluxes strengthen the entire Hadley cell (see Fig. 9c).

Apparently, the two limiting cases, that is,  $Q_c = 0$  and  $Q_c \neq 0$ , lead to vastly different conclusions on the

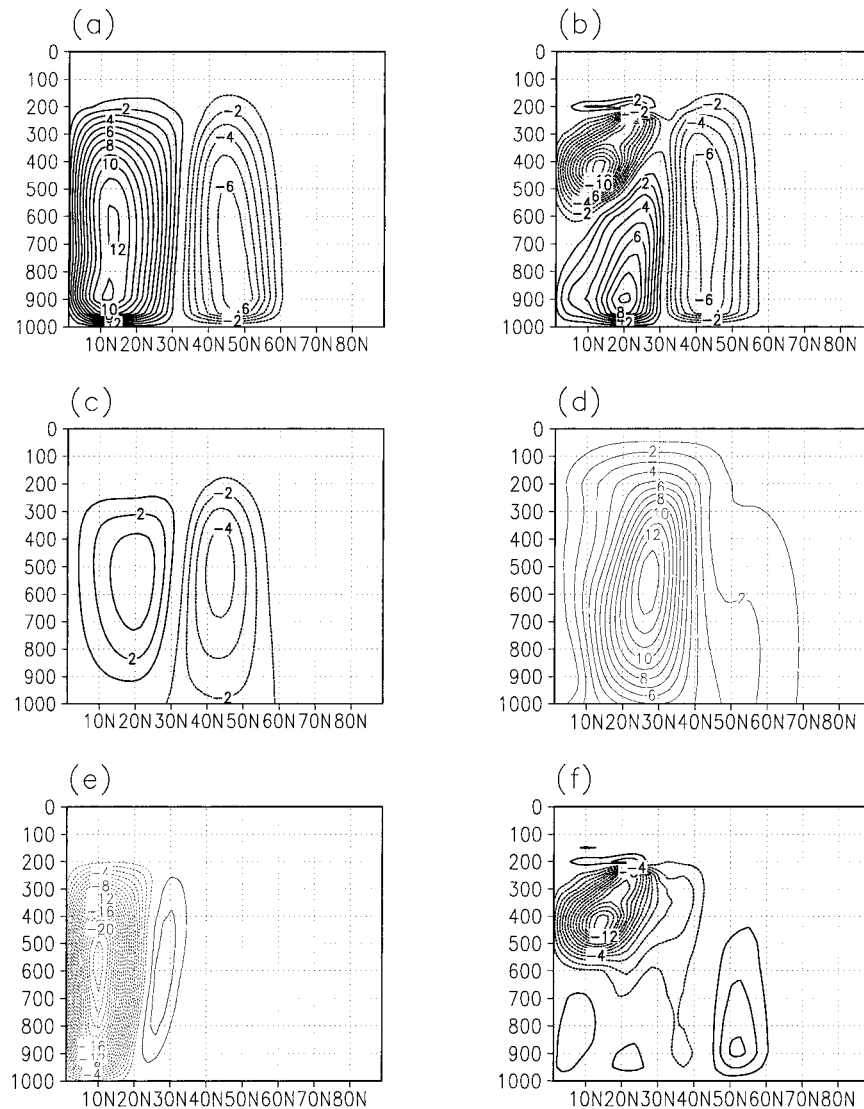


FIG. 9. For the nonaxisymmetric circulation with additional heating,  $Q_c$ , (a) QG diagnostic mass streamfunction; (b) eddy-driven mass streamfunction obtained from PE models; QG mass streamfunction responses to (c) eddy momentum and heat fluxes; (d) eddy diabatic heating; (e) eddy-induced static stability change on the axisymmetric circulation; and (f) effect of vertical and horizontal mixing of  $\Theta$  [the last two terms on (5)]. Contour interval is  $1 \times 10^{10} \text{ kg s}^{-1}$  for (a), (b), (c), and (f) and  $1 \times 10^9 \text{ kg s}^{-1}$  for (d) and (e). Dotted lines indicate negative values and zero contours are omitted.

role of the eddy fluxes. So, which case is more relevant for the atmosphere? We believe that the atmosphere falls somewhere between the  $Q_c = 0$  and  $Q_c \neq 0$  cases. This is because while the timescale of the convective heating is much shorter than that of the radiative heating, convective activity is also influenced by large-scale motion (see Arakawa 1993, Emanuel et al. 1994, and Neelin 1997 for reviews). By formulating the convective heating with a constant heating representation, one implicitly assumes that the convective heating occurs regardless the state of the ambient large-scale flow. This difficulty also arises from the fact that the net effect of the

eddies is to bring the axisymmetric circulations Hadley cells closer to the observed value. In other words, the eddy fluxes either intensify or dampen the axisymmetric circulations Hadley cell, so that in the nonaxisymmetric counterpart the Hadley cell strength takes a more reasonable value than that in the axisymmetric circulation. For example, in the control case, the maximum value of  $\Psi$  is  $9 \times 10^9$  and  $4.5 \times 10^{10} \text{ kg s}^{-1}$  for the axisymmetric and nonaxisymmetric flows, respectively. On the other hand, with the nonzero  $Q_c$ , the corresponding values are  $22 \times 10^{10}$  and  $10 \times 10^{10} \text{ kg s}^{-1}$ , respectively. One implication of this result is that the sensitivity of

the climate response to tropical heating may be much less than what axisymmetric circulation theory predicts (e.g., Rind 1986).

Therefore, a proper inference of the role of the eddy fluxes on the atmospheric Hadley cell calls for a better parameterization of diabatic heating (e.g., see Satoh 1994; Dodd and James 1997) than radiative relaxation and a constant representation for convective heating.

The use of numerical experiments with and without the baroclinic waves, together with the diagnosis of the MMC, elucidates subtle, but significant impacts of baroclinic eddies on the Hadley cells. In particular, it can be misleading to treat some of the extratropical climate changes as a direct response to tropical diabatic heating anomalies. As demonstrated in this study, it may well be that some tropical diabatic heating anomalies are induced by anomalous extratropical eddy fluxes, pointing out the need for caution in trying to establish any causal relationship between tropical and extratropical dynamics and climate.

Last, we note that the effect of the viscosity on the Hadley cell in the axisymmetric flow (KL) is analogous to that of the eddy momentum flux in the nonaxisymmetric flow. Given that the eddy momentum flux plays a crucial role in driving the Hadley cell, it would not be surprising if an axisymmetric model, with an appropriate viscosity, can be tuned to produce a Hadley cell close to the observed one.

*Acknowledgments.* We thank Dr. Steven Feldstein for comments on an earlier version of this manuscript. Comments by Dr. Volkmar Wirth and an anonymous reviewer also improved this manuscript. This research was supported by the National Science Foundation through Grant ATM-9525977 and by the National Oceanic and Atmospheric Administration through Award NA86GP0260.

#### REFERENCES

- Arakawa, A., 1993: Closure assumptions in the cumulus parameterization problem. *The Representation of Cumulus Convection in Numerical Models of the Atmosphere, Meteor. Monogr.*, No. 46, Amer. Meteor. Soc., 1–15.
- Becker, E., G. Schmitz, and R. Geprägs, 1997: The feedback of mid-latitude waves onto the Hadley cell in a simple general circulation model. *Tellus*, **49A**, 182–199.
- Chang, E. K. M., 1996: Mean meridional circulation driven by eddy forcings of different timescales. *J. Atmos. Sci.*, **53**, 113–125.
- Crawford, S. L., and T. Sasamori, 1981: A study of the sensitivity of the winter mean meridional circulations to sources of heat and momentum. *Tellus*, **33**, 340–350.
- Dodd, J. P., and I. N. James, 1997: The impact of latent-heat release on the Hadley circulation. *Quart. J. Roy. Meteor. Soc.*, **123**, 1763–1770.
- Eliassen, A., 1951: Slow thermally or frictionally controlled meridional circulation in a circular vortex. *Astrophys. Norv.*, **5**, 19–60.
- Emanuel, K. A., J. D. Neelin, and C. S. Bretherton, 1994: On large-scale circulations in convecting atmospheres. *Quart. J. Roy. Meteor. Soc.*, **120**, 1111–1143.
- Haynes, P. H., and T. G. Shepherd, 1989: The importance of surface pressure changes in the response of the atmosphere to zonally symmetric thermal and mechanical forcing. *Quart. J. Roy. Meteor. Soc.*, **115**, 1181–1208.
- Kim, H., and S. Lee, 2001: Hadley cell dynamics in a primitive equation model. Part I: Axisymmetric flow. *J. Atmos. Sci.*, **58**, 2845–2858.
- Kuo, H.-L., 1956: Forced and free meridional circulations in the atmosphere. *J. Meteor.*, **13**, 561–568.
- Lindzen, R. S., and A. Y. Hou, 1988: Hadley circulations for zonally averaged heating centered off the equator. *J. Atmos. Sci.*, **45**, 2416–2427.
- Neelin, J. D., 1997: Implications of convective quasi-equilibrium for the large-scale flow. *The Physics and Parameterization of Moist Atmospheric Convection*, R. K. Smith, Ed., NATO ASI Series, Series C, Vol. 505, Kluwer Academic, 413–446.
- Oort, A. H., and E. M. Raussmussen, 1970: On the annual variation of the monthly mean meridional circulation. *Mon. Wea. Rev.*, **98**, 423–442.
- Peixoto, J. P., and A. H. Oort, 1992: *Physics of Climate*. AIP Press, 520 pp.
- Pfeffer, R. L., 1981: Wave-mean flow interactions in the atmosphere. *J. Atmos. Sci.*, **38**, 1340–1359.
- Plumb, R. A., 1982: Zonally symmetric Hough modes and meridional circulations in the middle atmosphere. *J. Atmos. Sci.*, **39**, 983–991.
- Rind, D., 1986: The dynamics of warm and cold climates. *J. Atmos. Sci.*, **43**, 3–24.
- Satoh, M., 1994: Hadley circulations in radiative–convective equilibrium in an axially symmetric atmosphere. *J. Atmos. Sci.*, **51**, 1947–1968.